sciendo

Polish Journal of Chemical Technology, 26, 2, 1—7, 10.2478/pjct-2024-0011

Preparation of Nano Membranes with Triethylenetetramine Dihydrochloride (TETA-DH) and Multiwalled Carbon Nanotubes (MWCNT) for Seawater Desalination

Ahmed Alghamdi*

Department of Chemical Engineering Technology, Yanbu Industrial College, Royal, Commission Yanbu Colleges & Institutes, P.O. Box 30346, Yanbu Industrial City, 41912, Saudi Arabia

*Corresponding author: e-mail: alghamdia1@rcjy.edu.sa

Seawater Desalination uses hydrophobic membranes. Many techniques have been developed to improve membrane hydrophobicity by depositing particles on the membrane surface. In this study, a nanocomposite membrane utilizing Triethylenetetramine (TETA) is suggested. The membrane incorporates Multiwalled Carbon Nanotubes (MWCNT) in conjunction with Triethylenetetramine Dihydrochloride (TETA-DH). In water bath, different percentages of TETA-DH films are formed. Electro-spin fabrication of MWCNTs using TETA-DH yields smooth, low-pore membranes. Membranes and their characteristics are identified by contact angle, layer thickness, and conductivity measurements. Membrane performance is examined for heat flux and salt rejection. Compared to commercial membranes, the proposed membrane exhibits superior antifouling and anti-wetting features. The membrane exhibited permeation and rejection ratio of 46 Kg m^2 h^{-1} and 99.99% respectively which is superior as compared with other membranes. The hydrophilic Surface Modifying Macromolecules percentage (LSMM%) is evaluated because it depends on average pore size, hydrophobicity, surface porosity, and shape. The tests demonstrate the excellent performance of the proposed membrane for controlling membrane fouling.

Keywords: Multiwalled carbon nanotubes (MWCNT), Triethylenetetramine dihydrochloride (TETA-DH), Contact angle, and Foulant layer thickness.

INTRODUCTION

There is a need for a cost-effective water purification method that can effectively address the challenges of freshwater salination and other forms of contamination. Therefore, it is essential to implement a water purifying system that is economical in terms of cost[1]. For this purpose, several water treatment technologies are presented and applied, which fall under the primary, secondary, and tertiary categories[2]. Filtration, separation, coagulation, screening, centrifugation, sedimentation, coagulation, and flocculation are the primary technologies. Aerobic as well as anaerobic treatments are secondary technologies. Crystallization, solvent extraction, precipitation, Reverse Osmosis (RO), Ultrafiltration (UF), adsorption, electrodialysis, distillation, evaporation, oxidation, ion exchange, Nanofiltration (NF), Microfiltration (MF), and electrolysis are the tertiary technologies. Nevertheless, most of these technologies cannot fix water pollutants effectively[3].

Membrane-based desalination (MD) has been used very commonly compared with these techniques owing to its low cost and effective nature. In Membrane desalination, feed water is forced onto the membrane surface, which selectively passes water and retains salts. Among more types of membranes, remarkably higher water permeability along with salt rejection is achieved by the Polyamide RO (PA-RO) membranes; thus, it has become a chief technology to address water shortages via processes like sea-water desalination (SD) and wastewater reuse[4, 5].

In recent times, significant attention has been attracted by Carbon Nanotubes (CNTs) to synthesize membranes with attractive features for water purification. CNTs have been examined by recent studies to enhance stability and decrease production costs owing to their high mechanical stability, huge surface area, and interconnected pore structure[6]. Skuse et al. suggested a life cycle study to assess the SD's RO and MD environmental consequences from Graphene Oxide (GO)-enriched membranes. Most categories favored the RO-GO method over MD-GO due to reduced effects. It was unreliable for all GO membrane production systems since it only investigated one method[7]. Essalhi et al. introduced Direct Contact Membrane Distillation (DCMD) to characterize performance. Dual-layered Mixed Matrix Electrospun Nanofibrous Membranes (MM-ENMs) with a thin hydrophobic layer and a thick hydrophilic support layer reduced water vapor transport resistance and improved single-layer DCMD performance[8]. J. Fu et al. presented an as-prepared ZIF-8 in the existence of SiO_2@CNTs (ZFC) model that was combined into sulfonated poly (ether ether ketone) (SPEEK) for fabricating a series of composite proton exchange membranes. The results showed that the voltage of the Direct Methanol Fuel Cells (DMFC) equipped with SPEEK/ZSC-0.5 decreased by 9.2% during test[9]. H. Fu et al. established the well-structured 3D water channels featuring regular along with negatively-charged properties in the GO/SiO_2 composite membrane through in situ close-packing assembly of SiO_2 nanoparticles onto GO nanosheets. The presented technique attained high negative-charged dye molecules of 7.2%[10]. Yan et al. proffered a simple superhydrophobic ENM surface coating technology. Sprayed electrospun nanofiber membranes were fabricated. After spraying ENM, it was heat-pressed below the melting point. The membranes were superhydrophobic due to CNTs' increased hydrophobicity and reduced surface energy. With constant Vacuum MD (VMD) performance for over 26 hours, the 20 g/m^2 CNTs coated membrane had the highest water flow (28.4 kg/m^2h)[11].

In previous studies, the CNTs' usage in various separation techniques is facilitated by their thermal stability

along with controllable pore diameter. Chemical vapor deposition (CVD) techniques, which are economically viable, are involved in the CNTs[12, 13]. Nevertheless, for nanotube fabrication, the usage of substrates and templates is limited by the CVD techniques. The carbon and aromatic hydrocarbons easily contaminate the CNT membranes, which are harmful in large-scale production processes[14]. Also, achieving the CNT membranes' production of uniform as well as homogeneous structures on a large scale is difficult, thus posing a threat to commercialization[15]. To overcome all these issues, a new method is proposed for the preparation and characterization of a polymer membrane with CNTs for wastewater purification. This method uses Triethylenetetramine (TETA) as a membrane with added LSMM to overcome the contamination problems. Also, to overcome the nanotube fabrication issues, ultra-nanofiltration is utilized.

MATERIALS AND METHODS

Chemicals

For this study, chemicals were purchased from NM Enterprises Banglore and Luna Chemicals Surat. Chemicals purchased are MWCNT, sulphuric acid, Triethylenetetramine ($C_6H_{18}N_4$), thionyl chloride ($SOCl_2$), nitric acid, dimethyl formamide, and isopropyl alcohol. The Foulant used here were LSMM and Bovine Serum Albumin (BSA). Fig. 1 displays the LSMM's chemical structure, which is end-capped by an -OH bond that is attractive to the water molecules owing to its polar nature.

The membrane that was used for polymer formation was Emulsion poly (vinyl chloride) (PVC). Solvents, namely Polyethylene glycol additive (6000 g/mol) and N- Methylpyrrolidone were purchased from Kayaran Solvents, Chennai. These solvents were analyzed to have a purity of 99% by Solvent purity assay with GC-FID as well as Karl Fischer systems. By evaluating the sample with GC-FID and comparing the area of the solvent signal to the combined area of all peaks, determination is carried out. The solvent's concentration in the sample is represented as a percentage (%).

The membrane surface was mostly used for SD process applications. In this application, for deionizing water, iron chloride hexahydrate ($FeCl_3 \cdot 6H_2O$) was used. $FeCl_3 \cdot 6H_2O$ was analyzed for purity of 97%. For making final stock concentrations, $FeCl_3 \cdot 6H_2O$ was dissolved in water. This concentration ranges from 1000 mg/L. Sodium hypochlorite (NaOCl) was taken for oxidizing. NaOCl was analyzed to have chlorine not less than 5.2%. With Distilled Water (DW), NaOCl was diluted. This process continues until 1000 mg/l of stock concentration.

Synthesis

The Poly-MWCNT's nanocomposites are synthesized by oxidation polymerization. By utilizing ammonium persulfate as a redox initiator, aniline monomer's Chemical Oxidative Polymerization (COP) prepared the Poly-MWCNT. Primarily, Ammonium Peroxydisulfate (APS) along with P-toluene sulfonic Acid (PTSA) were dissolved separately in DW. Then, the PTSA solution was added to the APS solution that was stirred for 15 minutes. A mixture of 125 mL DW, 5 mL pyrrole, and 0.048 g of Poly-MWCNT was made and sonicated for 10 minutes. Then, the suspended solution was added to the APS/PTSA mixture, which was stirred for 4 hours at room temperature. Afterward, the prepared mixture was centrifuged. At 60 °C, the solid phase was separated and dried in a vacuum oven for 48 hours. The $SOCl_2$ residue was removed by evaporation. Then, at room temperature, the acquired black solid was dried in a vacuum oven. With 120 mL of TETA, the resulting solid was reacted for 96 hours at 120 °C and was washed with pure ethanol to remove excess TETA.

Preparation of membranes

A phase inversion technique was utilized for preparing 1% TETA-DH membranes. Different loadings of Poly-MWCNT for 0.0, 0.05, 0.1, 0.25, 0.5, and 1 wt% mixed through higher affinity betwixt solvent N-Methylpyrrolidone (NMP), PVC (15 wt%) as a major polymer and PEG (4 wt%) as a pore former and a hydrophilic additive were sensibly added to NMP. For 24 hours, the solution was mixed at room temperature. Then, to get rid of air bubbles, the solution of the cast was drained into an ultrasonic bath for 30 minutes. In neat glass plates, the solutions were formed utilizing a cast knife with 170 μm thickness and quickly immersed into a coagulation bath of DW at the temperature of 25 °C. After coagulation, for 24 hours, the membranes were soaked in a further DW bath to eliminate the remaining NMP, with hydrophobic Surface-Modifying Macromolecules (BSMM) as the last step of fabrication, Fig. 2 showed the proposed model.

Characterization of membrane

An optical profiler from RDS Industrial Solutions, Chennai detected the membrane surface roughness. For measuring the contact angle and surface energy, a contact angle analyzer was used (sessile drop method). The data in this signifies the average, plus/minus standard deviation after repeating the measurements 3 times. For analyzing the pore size distribution of membranes, a porometer machine (PoroLux™ 1000) was utilized from Concord Scientific Devices based in Chennai, India. For calculating membrane porosity, the gravimetric technique that involves a volume of 1-butanol in every single sample was utilized. For measuring thermal stability, a differential scanning calorimeter (DSC-Q200) was utilized, which measures how a sample's physical properties change along with temperature against time.

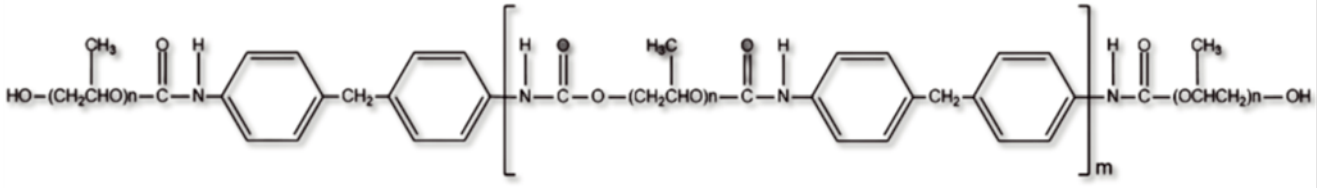

Figure 1. Chemical structure of LSMM

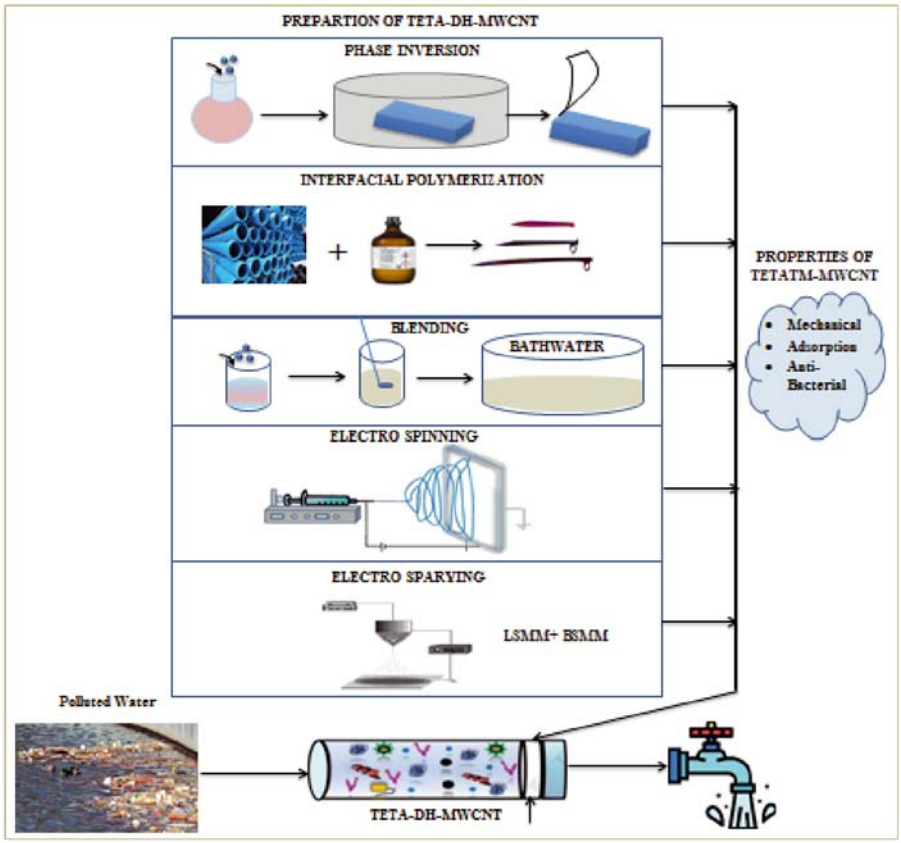

Figure 2. Flow diagram of the proposed model

Samples of approximately 10 mg in size were heated from room temperature (25 °C) to 300 °C at a heating rate of 10 °C per minute under nitrogen atmospheres (flow rate of 50 ml. min^{-1}).

Direct Contact membrane distillation (DCMD) tests

DCMD tests were executed on a laboratory-scale setup. The viability of using membrane distillation (MD) for the desalination of seawater and treatment of industrially discharged wastewater with high salinity was evaluated. Concentrated brines are produced and discharged during desalination. To prevent undesired crystallization inside the module along with the tubing, optimization is required for the viable MDC process's development and also for performing distillation tests. Therefore, selecting suitable MDs as well as crystallization operating conditions is essential. The parameters enclose flow rates, process temperature, duration of crystallization, and solution supersaturation. Initially, the flow rate of the permeate side was controlled with an optimum value of 0.5L/min, and this setup used a portable conductivity tester (Range: 0 to 1990 μS/cm, Thermo Fisher Scientific Inc) for measuring the permeate solution's conductivity, and its flux was attained by computing the increase of weight on the permeate side. It was continued for 1 hour, and also the pore size was tested. The salt rejection rate ($S_{rejection}$) is given as,

$$S_{rejection} = \left(1 - \frac{E_d}{E_f}\right) \times 100\% \tag{1}$$

Where, E_d symbolizes the distillate's conductivity and E_f epitomizes the feed solution's conductivity. Likewise, the process temperature on this solution was given by υ, ω and ς , which are constants that were related to a specific substance, and the temperature is given as T_t and vapor pressure is given as P_v.

$$P_v(T_t) = e^{\left(\upsilon - \frac{\omega}{\zeta + T_t}\right)} \tag{2}$$

As per this equation, the pressure of vapor increased exponentially for temperature. Conversely, water flux remains directionally proportional to the temperature fended. Hence, salt rejection is performed in solution--affected feed temperature, which in turn increases water flux. Also, this increase in temperature decreases the solubility of $CaCO_3$ but increases the solubility of CO_2. Thus, the pH value increased, which caused the calcium carbonate crystallization. The precipitation of the carbonate reaction is given as,

$$2HCO_3^- + Ca^{2+} \rightarrow CaCO_3 + CO_2 + H_2O \tag{3}$$

When this reaction results in a stable calcium concentration, the perception is stopped, and then this temperature is fixed as the standard temperature. Now, crystallization is not affected by the addition of iron content. With the increase in iron concentration, the solution supersaturation decreased, and the inhibition effectiveness of iron increased. This process slowed down the crystal growth rate and resulted in large crystals. Hence, an evaluation of the time for crystallization is necessary. The time duration of crystallization was affected by the nucleation effect and supersaturation. For reducing polarization effects as well as membrane fouling, turbulence in the feed channel is increased by the feed recirculation. Moreover, higher recovery factors increase the feed salt concentration, thus lowering the water vapor pressure at the feed side and diminishing the evaporation efficacy. However, attaining 80% recovery is not possible in any MD systems without feed

recirculation. This further mitigates the boundary layer, thus enhancing the permeate flux. Temperature polarization as well as membrane fouling are reduced by the higher recirculation rate owing to the water turbulence enhancement, which ensures a stable water flux.

RESULTS AND DISCUSSION

The efficacy of the MWCNT approach implemented with TETA-DH was evaluated using MATLAB and afterwards compared, as briefly outlined in the following discussion.

Water contact angle of TETA-DH membranes

Contact angle remains a common measurement for predicting the material surface's hydrophobicity or else hydrophilicity properties[16]. Fig. 3 displays the fabricated membranes' contact angle outcomes. Contact angle measurement concerns the liquid's surface tension as well as the surface energy. For pure PVC materials having a common surface energy of 30.3 J, the contact angle is 103. Smaller surface energy should be attained to obtain a greater contact angle. By adding a TETA in MWCNT, the contact angle diminishes regularly. But, with the increase of TETA dosage, the contact angle increases.

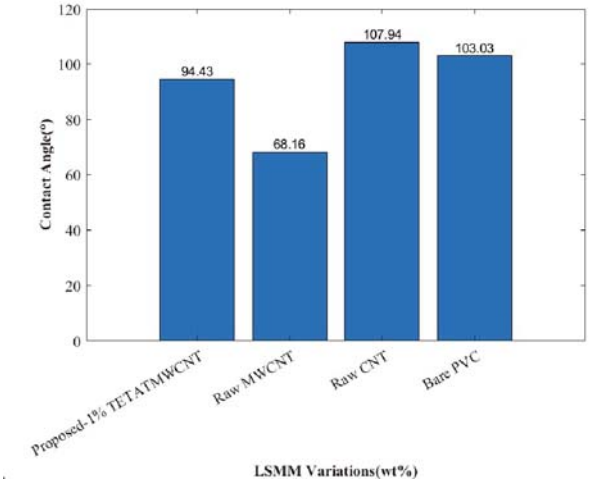

Figure 3. Contact angle representation

Owing to high porosity, the contact angle of the proposed membrane has increased up to 94.43, whereas other membranes like Raw MWCNT and Raw CNT have reached 68.16 and 107.94. The bare PVC reached 103.03 of contact angle. The hydrophilic agent was utilized by incorporating LSMM variation's varying concentrations and mixed in membrane preparation for MD desalination application. The minimum hydrophobicity value for MD (above 90°) is reached by the fabricated modified membranes since hydrophobic characteristics are required by the MD process to allow only vapor to pass the pores. Owing to the fluorine atoms, the contact angle is increased, thus creating lower surface tension and making them a hyperbolic membrane state[17]. The surface's excess wettability is averted by the BSMM's presence within the outer surface. Owing to the addition of LSMM, a slight reduction is indicated in contact angle value with the same amount of BSMM's coating agent.

Characteristics study of TETADH-MWCNT membrane

During dope solution preparation, the LSMM was mixed, and this exposed the white particles' presence on the pore surface. LSMM increased the membrane thickness concerning the proposed membrane's physical characteristics. The membrane thickness impacted both heat and mass with different correlations while implemented in the distillation process. Permutate flux was inversely proportional to the membrane thickness; a negative effect was created by this increase in thickness; also, lower flux was owing to the mass transfer resistance role. Concerning Table 1, the physical characteristics of the membrane played a role in high membrane thickness. Mass, as well as heat transfer coefficients with impact on membrane thickness, have a difference in correlation while employing the distillation process.

This work increased the membrane's thickness (25 to 50 μm), which was comparable with the range of commercial membranes for MD process (10 to 150 μm). During flux permeation, differentiating from the membrane effect occurs in which the thickness was obtained average owing to the membrane's mechanical strength. Casting solution viscosity maintained higher polymeric content, thereby restricting the molecular movement in the membrane. Hence, the number of pores in the membrane gets restricted. Thus, forming more pores in the membrane is difficult. Afterward, the membrane becomes strengthened and has thicker mechanical properties. The absorption performance is linked to the membrane's porosity, which lets air move through the membrane's inner side. The proposed membrane obtained an ideal porosity that meets the distillation specifications[18], which was a maximum of 90.97±2.34. Further, this works for an anti-bacterial and anti-fouling property that gives the membrane a longer lifetime.

Thermal Stability

MD processes need a high temperature that must be given for operation that is varied between 60° to 85°[19]. At this point, the membrane was evaluated for its thermal properties, and this was done by utilizing Differential Scanning Calorimetry (DSC). Also, based on the difference between heat flows, the function of temperature was measured. The melting point of the test shows a value of 161 °C, which was greater than in previous studies[20]. This was mainly owing to LSMM and also due to the TETA as the membrane augmented the material membrane's molecular weight that however influenced the melting point.

The endothermic peak on the thermogram curve is revealed in Fig. 4. This graph indicates the solid material's melting temperature. From this graph, it was interpreted that the 1% TETA-DH fabricated membrane that was implemented in this study has high thermal strength and

Table 1. Properties of membranes concerning Max load, Max tensile stress, average pore size, and overall porosity

Membrane	Max load (N)	Max tensile stress (N/cm^2)	Average pore size (μm)	Overall porosity (%)
TETADHWCNT	0.51 ± 0.04	1.40 ± 0.09	0.616 ± 0.065	90.97 ± 2.34
MWCNT	0.53 ± 0.03	1.64 ± 0.06	0.476 ± 0.134	86.12 ± 2.32
CNT	0.55 ± 0.05	1.71 ± 0.03	0.326 ± 0.105	84.11 ± 2.30

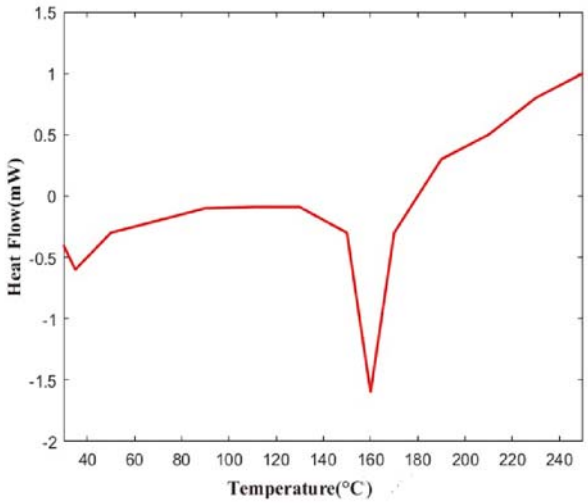

Figure 4. DSC thermogram of the membrane

they were constantly operating in a range between 60 to 90. From this result, the calculation has been made to find the average heat flow $\Delta H = -1.64$ mW with a melting temperature $T_m = 161$ °C.

DCMD performance

The prepared TETA-DH is evaluated for the DCDM test and then compared with the commercial hydrophobic membranes that were analytically estimated. With 3.5 wt% NaCl solution, the tests were executed at 60° as feed; also, the permeate side was retained at 20°. The permeate fluxes were calculated and shown in Table 2.

The parameter that quantifies the rate of water flow per unit surface area of a membrane, expressed as gallons per day per square foot (GPD/ft^2), and the resulting volume of treated water that flows through the membrane, is referred to as membrane flux[21]. The flux rate relies on the membrane sort and various physical as well as environmental operating conditions. Likewise, the amount of permeate produced per unit area of membrane surface per unit of time is named as the membrane's flux rate. In general, flux is represented as Gallons per square foot per Day (GFD) or else as cubic meters per square meter per day.

Table 2. Representation of permeate flux and average flux

Membrane	Initial flux (kg/m^{2}h)	Average Flux (kg/m^{2}h)
TETADHWCNT	20.88 ± 0.71	14.68 ± 1.27
Raw MWCNT	21.22 ± 0.82	16.12 ± 1.29
Raw CNT	33.26 ± 1.17	25.61 ± 1.31
Bare PVC	20.98 ± 0.63	15.61 ± 1.17
0.05% TETA	50.67 ± 1.81	24.68 ± 1.42
0.5% TETA	20.89 ± 0.81	13.88 ± 1.27

The fouling layer thickness vs. operation time graph compared with commercial membranes is exemplified in Fig. 5(a). The increase in fouling layer thickness increases the flow rate and decreases the flow resistance. Nevertheless, the flow rate of gas decreases owing to increased flow resistance; thus, it should be kept adequate and the operators were increased with the blowing membrane. The fluctuation of the flow rate was made stable at 50 μm. Due to low molecular weight and evaluation in varying time phases, the other membranes were much higher than 200 μm. Yet, the fouling rate, asymptotic value, and period are different in the later phase. This appears to rely on the ultimate difference in the operating conditions like temperatures as well as recirculation flow rate. Likewise, the permeate flux value versus time in a minute is demonstrated in Fig. 5(b). The flux of the proposed 1% TETA-DH MWCNT at varying periods obtained a stable permeate flux owing to the UF opted for spinning purposes and the tensile strength of the membrane.

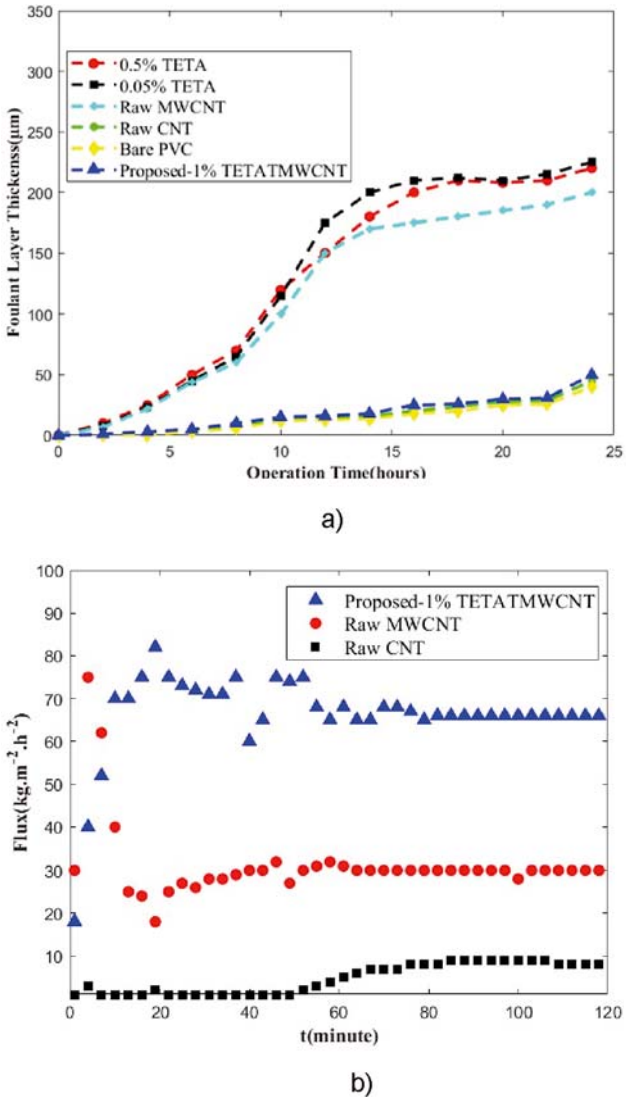

Figure 5. (a) Graphical representation of foulant layer thickness (left). (b) permeate flux (right)

For describing the antifouling property, the flux recovery ratio is used as shown in Fig. 6. Here, the FRR percentage values are plotted and these values are obtained from the proposed nanocomposite membranes. Now, the membranes, which were taken by utilizing TETA-DH, were employed. By using this membrane, MWCNT filters the protein, thereby reducing the RO content. For this purpose, the feed temperature was selected optimally utilizing the flux rate. For the varying periods, the flux rate was computed, and the amount of fouling was determined. Here, when compared to bare PVC membranes, commercial membranes show better FRR % values. The modified poly-MWCNT membrane has an increased flux rate of up to 76.1%, this was owing to ultra-nano filtration of CNTs. Overall, the performance of the tubes displayed better hydrophilicity value.

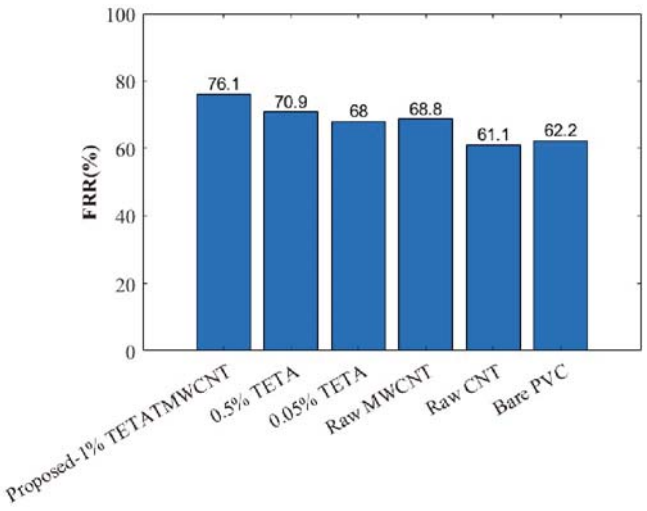

Figure 6. Graphical representation of the percentage of flux recovery ratio

Salt Rejection ratio

A measure of how well the passage of dissolved ions is rejected by a membrane element is named salt rejection[22]. Sodium chloride (NaCl) is utilized as a measurement standard even though an RO element might be called upon to reject numerous different ions. By utilizing the conductivity of feed water and the permeate water, salt rejection is calculated[23]. For the salt rejection, the conductivity of the feed is high; thus, the system performs well. Cleaning or else replacement is required for the membranes as indicated by the lower salt rejection.

The membrane's salt rejection ratio for saltwater and seawater is exemplified in Fig. 7. Owing to the existence of organic contamination in the seawater, LSMM wt% of the membrane for seawater is low, which causes the membrane's fouling and wetting. Still, the membrane obtained a 99.9% rejection ratio for both saltwater and seawater with an increase in LSMM content to the TETADH-MWCNT. The proposed membrane obtained a better salt rejection ratio due to the high hydrophobic properties of the membrane.

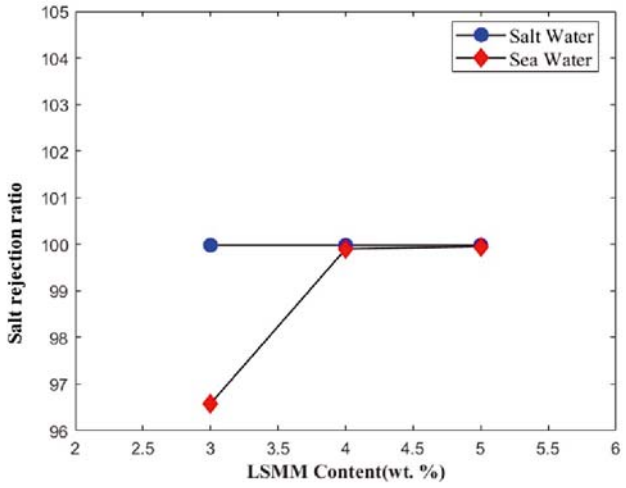

Figure 7. Salt rejection ratio Vs LSMM content

Table 3. Comparison of proposed and previous studies

Goal	Rejection %	Permeation (pressure)	Polymer	References
Improvement of antifouling	99.9	34.4760 Kgm^2h^{-1}	PVC	[8]
Lead removal from water	99.98	19.6060 Kgm^2h^{-1}	PVC	[25]
Dye rejection and antibacterial activity	99.9	–1.60 Kgm^2h^{-1}	PVC	[24]
Hydrophilic modification of PVC membranes with CNTs for improvement of salt rejection and fouling	99.99	46 Kgm^2h^{-1}	PVC	This study

Comparison with other studies

This research study was compared with previous studies that were similar to the objective of SD using MD, and depicted in Table 3. This displayed that the proposed study attained the objective with a standard level of permeation and rejection ratio of 46 Kg m^2 h^{-1} and 99.99%, whereas Qi et al.[24] obtained –1.60 Kg $m^2h^{-1}$and 99.9%, Xue et al.[25] obtained 19.6060 Kg m^2 h^{-1} and 99.98, and finally Essalhi and co-workers[8] obtained 34.4760 Kg m^2 h^{-1} and 99.9%, respectively. Therefore, the proposed study remains far better than the previous studies.

CONCLUSION

In this work, MWCNT, which was fabricated by employing electrospinning and electro-spraying mechanisms, was employed with 1% TETA-DH. Membrane fouling could be successfully mitigated by the TETA-DH membrane, thus enhancing desalination productivity in the distillation system. When contrasted with other commercial membranes, water flux, conductivity, and foulant layer thickness were maintained in the range of 14.68±1.27, 50um, and 76.1%, respectively. With a higher salt rejection ratio of 99.9%, the membrane showed a higher hydrophobic range under pretreatment. With a high regeneration ratio, the contact angle was recovered between 94.43. Therefore, during distillation operations, long-term stable performance could be achieved by the membranes coupled with appropriate pre-as well as post-treatment techniques such as oxidation, filtration, flocculation, coagulation, and adsorption; also, the operational costs related to membrane replacement could be reduced. Lastly, a stable anti-fouling distillation process design, which has a higher potential for economically feasible pilot-scale distillation system development, integrates renewable membranes.

LITERATURE CITED

1. Safaei, J., Xiong, P. & Wang, G. (2020). Progress and Prospects of Two-Dimensional Materials for Membrane-Based Water Desalination. *Mater. Today Adv. 8*, 100108. DOI: 10.1016/j.mtadv.2020.100108.

2. Ou, R., Zhang, H., Truong, V.X., Zhang, L., Hegab, H.M., Han, L., Hou, J., Zhang, X., Deletic, A., Jiang, L., Simon, G.P. & Wang, H. (2020). A Sunlight-Responsive Metal–Organic Framework System for Sustainable Water Desalination. *Nat. Sustain. 3*(12), 1052–1058. DOI: 10.1038/s41893-020-0590-x.

3. Ihsanullah, I. (2020). Potential of MXenes in Water Desalination: Current Status and Perspectives. *Nano-Micro Lett. 12*(1), 1–20. DOI: 10.1007/s40820-020-0411-9.

4. Lawal, D.U., Antar, M.A., Khalifa, A., Zubair, S.M. & Al-Sulaiman, F. (2020). Experimental Investigation of Heat Pump Driven Humidification-Dehumidification Desalination System for Water Desalination and Space Conditioning. *Desalination.475* (October 2019). DOI: 10.1016/j.desal.2019.114199.

5. Jie, G., Kongyin, Z., Xinxin, Z., Zhijiang, C., Min, C., Tian, C. & Junfu, W. (2015). Preparation and Characterization of Carboxyl Multi-Walled Carbon Nanotubes/Calcium Alginate Composite Hydrogel Nano-Filtration Membrane. *Mater. Lett. 157*, 112–115. DOI: 10.1016/j.matlet.2015.05.080.

6. Nitodas, S.F., Das, M. & Shah, R. (2022). Applications of Polymeric Membranes with Carbon Nanotubes: A Review. *Membranes (Basel). 12*(5). DOI: 10.3390/membranes12050454.

7. Skuse, C., Tarpani, R. R. Z., Gorgojo, P., Gallego-Schmid, A. & Azapagic, A. (2023). Comparative Life Cycle Assessment of Seawater Desalination Technologies Enhanced by Graphene Membranes. *Desalination.551*, 1–17. DOI: 10.1016/j.desal.2023.116418.

8. Essalhi, M., Khayet, M., Tesfalidet, S., Alsultan, M. & Tavajohi, N. (2021). Desalination by Direct Contact Membrane Distillation Using Mixed Matrix Electrospun Nanofibrous Membranes with Carbon-Based Nanofillers: A Strategic Improvement. *Chem. Eng. J. 426* (July), 131316. DOI: 10.1016/j.cej.2021.131316.

9. Fu, J., Ni, J., Wang, J., Qu, T., Hu, F., Liu, H., Zhang, Q., Xu, Z., Gong, C. & Wen, S. (2023). Highly Proton Conductive and Mechanically Robust SPEEK Composite Membranes Incorporated with Hierarchical Metal-Organic Framework/Carbon Nanotubes Compound. *J. Mater. Res. Technol. 22*, 2660–2672. DOI: 10.1016/j.jmrt.2022.12.118.

10. Fu, H., Wang, Z., Li, P., Qian, W., Zhang, Z., Zhao, X., Feng, H., Yang, Z., Kou, Z. & He, D. (2023). Well-Structured 3D Channels within GO-Based Membranes Enable Ultrafast Wastewater Treatment. *Nano Res. 16* (2), 1826–1834. DOI: 10.1007/s12274-022-4970-6.

11. Yan, K.K., Jiao, L., Lin, S., Ji, X., Lu, Y. & Zhang, L. (2018). Superhydrophobic Electrospun Nanofiber Membrane Coated by Carbon Nanotubes Network for Membrane Distillation. *Desalination. 437*, 26–33. DOI: 10.1016/j.desal.2018.02.020.

12. Ali, S., Rehman, S.A.U., Luan, H.Y., Farid, M.U. & Huang, H. (2019). Challenges and Opportunities in Functional Carbon Nanotubes for Membrane-Based Water Treatment and Desalination. *Sci. Total Environ. 646*(19), 1126–1139. DOI: 10.1016/j.scitotenv.2018.07.348.

13. Haghighat, N. & Vatanpour, V. (2020). Fouling Decline and Retention Increase of Polyvinyl Chloride Nanofiltration Membranes Blended by Polypyrrole Functionalized Multiwalled Carbon Nanotubes. *Mater. Today Commun. 23* (January 2019), 100851. DOI: 10.1016/j.mtcomm.2019.100851.

14. Amiri, S., Asghari, A., Vatanpour, V. & Rajabi, M. (2020). Fabrication and Characterization of a Novel Polyvinyl Alcohol-Graphene Oxide-Sodium Alginate Nanocomposite Hydrogel Blended PES Nanofiltration Membrane for Improved Water Purification. *Sep. Purif. Technol. 250* (May), 117216. DOI: 10.1016/j.seppur.2020.117216.

15. Manorma, Ferreira, I., Alves, P., Gil, M.H. & Gando-Ferreira, L.M. (2021). Lignin Separation from Black Liquor by Mixed Matrix Polysulfone Nanofiltration Membrane Filled with Multiwalled Carbon Nanotubes. *Sep. Purif. Technol. 260* (December 2020). DOI: 10.1016/j.seppur.2020.118231.

16. Ismail, M.F., Islam, M.A., Khorshidi, B., Tehrani-Bagha, A. & Sadrzadeh, M. (2022). Surface Characterization of Thin-Film Composite Membranes Using Contact Angle Technique: Review of Quantification Strategies and Applications. *Adv. Colloid Interface Sci. 299*, 102524. DOI: 10.1016/j.cis.2021.102524

17. Cai, J., Liu, X., Zhao, Y. & Guo, F. (2018). Membrane Desalination Using Surface Fluorination Treated Electrospun Polyacrylonitrile Membranes with Nonwoven Structure and Quasi-Parallel Fibrous Structure. *Desalination*. 429, 70–75. DOI: 10.1016/j.desal.2017.12.019

18. Ravi, J., Othman, M.H.D., Matsuura, T., Bilad, M.R., El-Badawy, T.H., Aziz, F., Ismail, A.F., Rahman, M.A. & Jaafar, J. (2020). Polymeric Membranes for Desalination Using Membrane Distillation: A Review. *Desalination.* 490, 114530. DOI: 10.1016/j.desal.2020.114530.

19. Zhao, S. & Zou, L. (2011). Effects of Working Temperature on Separation Performance, Membrane Scaling and Cleaning in Forward Osmosis Desalination. *Desalination.* 278(1–3), 157–164. DOI: 10.1016/j.desal.2011.05.018.

20. Rahman, M.S., Ahmed, M. & Chen, X.D. (2006). Freezing-melting Process and Desalination: I. Review of the State-of-the-art. *Sep. Purif. Rev.* 35(02), 59–96. DOI: 10.1080/15422110600671734.

21. Alklaibi, A.M. & Lior, N. (2005). Membrane-Distillation Desalination: Status and Potential. *Desalination.* 171(2), 111–131. DOI: 10.1016/j.desal.2004.03.024.

22. Wang, Q., Li, N., Bolto, B., Hoang, M. & Xie, Z. (2016). Desalination by Pervaporation: A Review. *Desalination.* 387, 46–60. DOI: 10.1016/j.desal.2016.02.036.

23. Padaki, M., Isloor, A.M., Ismail, A.F. & Abdullah, M.S. (2012). Synthesis, Characterization and Desalination Study of Novel PSAB and MPSAB Blend Membranes with Polysulfone (PSf). *Desalination*. 295, 35–42. DOI:10.1016/j.desal.2012.03.014.

24. Qi, P., Zhao, C., Wang, R., Fei, T. & Zhang, T. (2018). High-Performance QCM Humidity Sensors Using Acidized-Multiwalled Carbon Nanotubes as Sensing Film. *IEEE Sens. J.* 18(13), 5278–5283. DOI: 10.1109/JSEN.2018.2839110.

25. Xue, G., Chen, Q., Lin, S., Duan, J., Yang, P., Liu, K., Li, J. & Zhou, J. (2018). Highly Efficient Water Harvesting with Optimized Solar Thermal Membrane Distillation Device. *Glob. Challenges.* 2(5–6), 1800001. DOI: 10.1002/gch2.201800001.